Activation of Hydrogen and Related Small Molecules by the Unsaturated Cluster Complex $PtOs_3(CO)_7(PBu^t_3)(\mu\text{-}PBu^t_2)(\mu_4\text{-}CHCMeCH)$

Richard D. Adams,*[,†] Erin M. Boswell,[†] Michael B. Hall,*[,‡] and Xinzheng Yang[‡]

Department of Chemistry and Biochemistry, University of South Carolina, Columbia, South Carolina 29208, and Department of Chemistry, Texas A&M University, College Station, Texas 77843-3255

Received May 22, 2008

Reactions of the unsaturated mixed metal cluster complex $PtOs_3(CO)_7(PBu^t_3)(\mu\text{-}PBu^t_2)(\mu_4\text{-}CHCMeCH)$, **1**, with hydrogen, $HGePh_3$, and PhC_2H have been investigated. Compound **1** reacts reversibly with hydrogen at room temperature to yield the dihydrido complex $PtOs_3(CO)_7(PBu^t_3)(\mu\text{-}PBu^t_2)(\mu_4\text{-}CHCMeCH)(\mu\text{-}H)(H)$, **2**. A computational analysis shows that the hydrogen addition occurs by oxidative addition at the electronically unsaturated platinum atom and passes through two unstable intermediates before giving the final product **2**. Compound **1** reacts with $HGePh_3$ at the Ge−H bond to form the complex $PtOs_3(CO)_7(PBu^t_3)(\mu\text{-}PBu^t_2)(\mu_4\text{-}CHCMeCH)(GePh_3)(\mu\text{-}H)$, **3**, but in this reaction the $HGePh_3$ addition occurred at one of the osmium atoms and a CO ligand was shifted to the platinum atom. Compound **1** reacts with PhC_2H by loss of the platinum atom and the PBu^t_3 ligand to give the compound $Os_3(CO)_7(\mu\text{-}PBu^t_2)[\mu_3\text{-}\eta^5\text{-}CHCMeC(H)CCPhH]$, **4**. In the process, the PhC_2H molecule became bonded to the CHCMeCH ligand in **1** and its hydrogen atom was shifted to the phenyl-substituted carbon atom to form a triply bridging CHCMeC(H)CCPhH ligand. All of the products were characterized by single-crystal X-ray diffraction analyses.

Introduction

Today, there is considerable interest in developing hydrogen as a means to store and utilize energy.[1] Catalysts will be required to facilitate the formation of hydrogen and its safe utilization in any futuristic hydrogen economy.[2] The most efficient and safe catalysts for hydrogen utilization are based on the platinum group metals.[2] Molecules and materials that can reversibly absorb large quantities of hydrogen are also of interest for its safe storage.[3,4] Although there has been much study of the activation of hydrogen by mononuclear metal complexes,[5] there are relatively few examples of reversible additions of hydrogen to polynuclear metal complexes that are not accompanied by the addition and elimination of other ligands.[6−10] We and others have been employing highly sterically crowded phosphine ligands to create unsaturation in polynuclear metal complexes for the purpose of activating hydrogen under mild conditions.[7−10] We have recently reported the unsaturated dirhenium–diplatinum complex $Pt_2Re_2(CO)_7(PBu^t_3)_2(\mu\text{-}H)_2$, which contains two very

* Corresponding author. E-mail: adams@mail.chem.sc.edu.
† University of South Carolina.
‡ Texas A&M University.

(1) (a) *A Multiyear Plan for the Hydrogen R&D Program: Rationale, Structure, and Technology Road Maps*; U.S. Department of Energy: Washington, DC, 1999; http://www.eere.energy.gov/hydrogenandfuelcells/pdfs/bk28424.pdf, p 32. (b) *National Hydrogen Energy Road Map*; U.S. Department of Energy: Washington, DC, 2002; http://www.sc.doe.gov/bes/reports/files/NHE_rpt.pdf, p 17. (c) Ogden, J. M. *Phys. Today* **2002**, *55*, 69–75. (d) Ogden, J. M. *Annu. Rev. Energy Environ.* **1999**, *24*, 227–279. (e) Ogden, J. *Sci. Am.* **2006**, *295*, 94–101. (f) Crabtree, G. W.; Dresselhaus, M. S. *MRS Bull.* **2008**, *33*, 421–428. (g) Sigfusson, T. I. *Phil. Trans. R. Soc. A* **2007**, *365*, 1025–1042. (h) Edwards, P. P.; Kuznetsov, V. L.; David, W. I. F. *Phil. Trans. R. Soc. A* **2007**, *365*, 1043–1056.

(2) (a) Farruato, R. J.; Liu, Y.; Ruettinger, W.; Ilinich, O.; Shore, L.; Giroux, T. *Catal. Rev.* **2007**, *49*, 141–196. (b) Adams, R. D.; Captain, B. *Angew Chem., Int. Ed.* **2008**, *47*, 252–257. (c) Thomas, J. M.; Raja, R.; Johnson, B. F. G.; Hermans, S.; Jones, M. D.; Khimyak, T. *Ind. Eng. Chem. Res.* **2003**, *42*, 1563–1570. (d) Armor, J. N. *Catal. Lett.* **2005**, *101*, 131–135.

(3) (a) Schlapbach, L.; Züttel, A. *Nature* **2001**, *414*, 353–358. (b) Zecchina, A.; Borgida, S.; Vitillo, J. G.; Ricchiardi, G.; Lamberti, C.; Spoto, G.; Bjørgen, M.; Lillerud, K. P. *J. Am. Chem. Soc.* **2005**, *127*, 6361–6366. (c) Nijkamp, M. G.; Raaymakers, J. E. M. J.; van Dillen, A. J.; de Jong, K. P. *Appl. Phys. A: Mater. Sci. Process.* **2001**, *72*, 619–623. (d) Weitkamp, J.; Fritz, M.; Ernst, S. *Int. J. Hydrogen Energy* **1995**, *20*, 967–970.

(4) (a) Rosi, N. L.; Eckert, J.; Eddaoudi, M.; Vodak, D. T.; O'Keerre, M.; Yaghi, O. M. *Science* **2003**, *300*, 1127–1129. (b) Zhao, X.; Xiao, B.; Fletcher, A. J.; Thomas, K. M.; Bradshaw, D.; Rosseinsky, M. J. *Science* **2004**, *306*, 1012–1015. (c) Rowsell, J. L. C.; Eckert, J.; Yaghi, O. M. *J. Am. Chem. Soc.* **2005**, *127*, 14904–14099. (d) Rowsell, J. L. C.; Spencer, E. C.; Eckert, J.; Howard, J. A. K.; Yaghi, O. M. *Science* **2005**, *309*, 1350–1354. (e) Rowsell, J. L. C.; Yaghi, O. M. *Angew. Chem., Int. Ed.* **2005**, *44*, 4670–4679. (f) Dinca, M.; Long, J. R. *J. Am. Chem. Soc.* **2005**, *127*, 9376–9377. (g) Kaye, S. S.; Long, J. R. *J. Am. Chem. Soc.* **2005**, *127*, 6506–6507. (h) Sun, D.; Ma, S.; Ke, Y.; Collins, D. J.; Zhou, H.-C. *J. Am. Chem. Soc.* **2006**, *128*, 3896–3897.

(5) Kubas, G. J. *Metal Dihydrogen and σ-Bond Complexes*; Kluwer/Academic/Plenum Publishers: New York, 2001.

(6) (a) Gray, T. G.; Veige, A. S.; Nocera, D. G. *J. Am. Chem. Soc.* **2004**, *126*, 9760–9768. (b) Farrugia, L. J.; Green, M.; Hankey, D. R.; Orpen, A. G.; Stone, F. G. A. *J. Chem. Soc., Chem. Commun.* **1983**, 310–312. (c) Adams, R. D.; Wang, S. *Organometallics* **1986**, *5*, 1272–1274. (f) Aubart, M. A.; Chandler, B. D.; Gould, R. A. T.; Krogstad, D. A.; Schoondergang, M. F. J.; Pignolet, L. H. *Inorg. Chem.* **1994**, *33*, 3724–3734. (d) Safarowic, F. J.; Bierdeman, D. J.; Keister, J. B. *J. Am. Chem. Soc.* **1996**, *118*, 11805–11812. (e) Arif, A. M.; Bright, T. A.; Jones, R. A.; Nunn, C. M. *J. Am. Chem. Soc.* **1988**, *110*, 6894–6895.

(7) Adams, R. D.; Captain, B.; Smith, M. D.; Adams, R. D.; Captain, B.; Mark, D. Smith.; Beddie, C.; Hall, M. B. *J. Am. Chem. Soc.* **2007**, *129*, 5981–5991.

(8) Adams, R. D.; Captain, B.; Beddie, C.; Hall, M. B. *J. Am. Chem. Soc.* **2007**, *129*, 986–1000.

(9) Adams, R. D.; Captain, B.; Zhu, L. *J. Organomet. Chem.* **2008**, *693*, 816–833.

(10) (a) Brayshaw, S. K.; Ingleson, M. J.; Green, J. C.; McIndoe, J. S.; Raithby, P. R.; Kociok-Köhn, G.; Weller, A. S. *J. Am. Chem. Soc.* **2006**, *128*, 6247–6263. (b) Brayshaw, S. K.; Ingleson, M. J.; Green, J. C.; Raithby, P. R.; Kociok-Köhn, G.; McIndoe, J. S.; Weller, A. S. *Angew. Chem., Int. Ed.* **2005**, *44*, 6875–6878. (c) Ingleson, M. J.; Mahon, M. F.; Raithby, P. R.; Weller, A. S. *J. Am. Chem. Soc.* **2004**, *126*, 4784–4785.

10.1021/om800467v CCC: $40.75
Publication on Web 09/05/2008

bulky tri-tert-butylphosphine ligands. This compound adds 1 equiv of H_2 at room temperature to yield the tetrahydrido complex $Pt_2Re_2(CO)_7(PBu^t_3)_2(\mu\text{-}H)_4$ (eq 1).[7] The added H_2 can then be removed by heating the compound to 97 °C. The dirheniumtriplatinum complex, $Pt_3Re_2(CO)_6(PBu^t_3)_3$ sequentially adds up to 3 equiv of H_2 at room temperature in a process that is partially photoreversible (eq 2).[8]

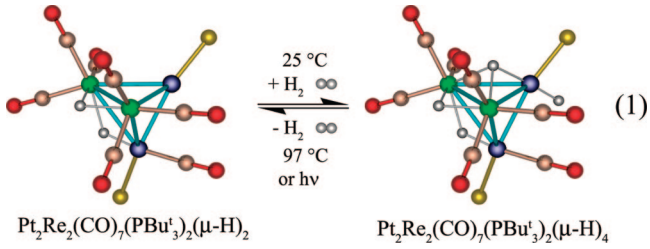

(1)

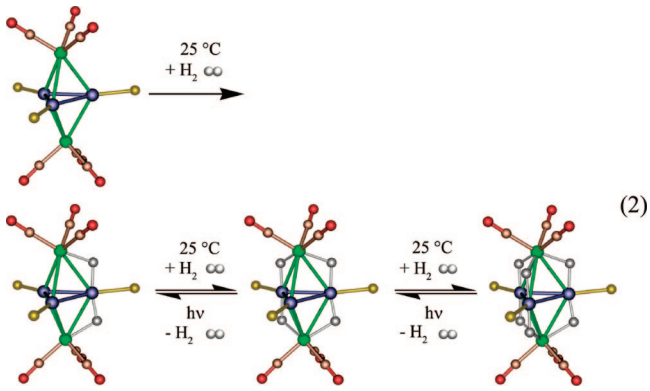

(2)

The compound $Pt_2Os_3(CO)_{10}(PBu^t_3)_2$ sequentially and reversibly adds 2 equiv of hydrogen at 0 °C, but does so by the breaking and making of some of the Pt−Os bonds (eq 3).[9]

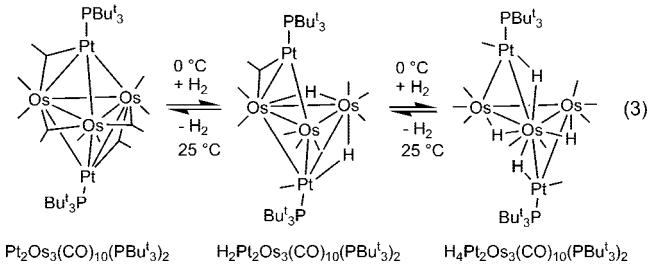

(3)

Weller and co-workers have reported an interesting family of hydridohexarhodium complexes $[Rh_6(PR_3)_6H_{12}][BAr^F_4]_2$ (R = ^{i}Pr, Cy; Ar^F = $[B\{C_6H_3(CF_3)_2\}_4]$)[4] that add an additional 2 equiv of hydrogen, reversibly, to yield the hexadecahydride complexes $[Rh_6(PR_3)_6H_{16}][BAr^F_4]_2$ (R = ^{i}Pr, Cy; Ar^F = $[B\{C_6H_3(CF_3)_2\}_4]$).[10]

We have recently reported the synthesis and structural analysis of the new unsaturated platinum−osmium cluster complex $PtOs_3(CO)_7(PBu^t_3)(\mu\text{-}PBu^t_2)(\mu_4\text{-}CHCMeCH)$, **1**.[11] Compound **1** has a total of 58 cluster valence electrons and is thus electron deficient by the amount of four electrons. Compound **1** has been found to add CO reversibly at its platinum atom.[11] We have now investigated the reactions of **1** with hydrogen as well as with $HGePh_3$ and PhC_2H. The results of these studies are reported here.

Experimental Section

General Data. All the reactions were performed under a nitrogen atmosphere using Schlenk techniques. Reagent grade solvents were dried by the standard procedures and were freshly distilled prior to use. Infrared spectra were recorded on an AVATAR 360 FT-IR spectrophotometer. ^{1}H NMR and ^{31}P{^{1}H} NMR were recorded on a Varian Mercury 400 spectrometer operating at 400 and 162 MHz, respectively. ^{31}P{^{1}H} NMR spectra were externally referenced against 85% *ortho*-H_3PO_4. Positive ion mass spectra for **1** and **4** were recorded on a Waters Micromass Q-T quadrupole time-of-flight instrument by using electrospray (ES) ionization. Mass spectra of **2** and **3** were obtained by direct exposure probe using electron impact ionization (EI) performed on a VG 70S instrument. Compound **1** was prepared as previously reported.[11] Triphenylgermane and phenylacetylene were purchased from Aldrich and were used without further purification. Product separations were performed by TLC in air by using Analtech 0.25, 0.5, and 1.0 mm silica gel 60 Å F_{254} glass plates.

Reaction of 1 with H_2. A 7.0 mg (0.005 mmol) amount of **1** was dissolved in 10 mL of distilled hexane in a 50 mL three-neck flask. The solution was purged with hydrogen gas for 2 h at room temperature. The solution turned from brown to orange. The solvent was then removed in vacuo and the residue was extracted with methylene chloride, applied to TLC plates, and separated by eluting with a 4:1 (v/v) hexane/methylene chloride solvent mixture to yield in order of elution 5.1 mg (72%) of orange $PtOs_3(CO)_7(PBu^t_3)(\mu\text{-}PBu^t_2)(\mu_4\text{-}CHCMeCH)(\mu\text{-}H)(H)$, **2**, and 1.5 mg (21%) of unreacted **1**. Spectral data for **2**: IR (cm^{-1} in CH_2Cl_2): 2064(s), 2053(w), 1994(vs), 1979(s), 1965(s), 1926(m), 1900(w). ^{1}H NMR ($C_6D_5CD_3$ in ppm, −60 °C): δ −15.62 (s, 1H, $^1J_{Pt-H}$ = 443 Hz), −12.82 (d, 1H, $^1J_{Pt-H}$ = 1285 Hz, $^2J_{P-H}$ = 16 Hz), 0.845 (s, 36H, br), 2.24 (s, 3H), 3.64 (d, 1H, $^3J_{P-H}$ = 2 Hz), 8.30 (d, 1H, $^3J_{P-H}$ = 2 Hz). ^{1}H NMR ($C_6D_5CD_3$ in ppm, +20 °C): δ −15.8 (s, 1H, broad), −13.7 (s, 1H, br), 0.951 (d, 27H, $^3J_{P-H}$ = 12 Hz), 1.00 (d, 9H, $^3J_{P-H}$ = 12 Hz), 1.33 (d, 9H, $^3J_{P-H}$ = 14 Hz), 2.36 (s, 3H), 3.81 (d, 1H, $^3J_{P-H}$ = 2 Hz), 8.51 (dd, 1H, $^3J_{P-H}$ = 2 Hz, $^3J_{P-H}$ = 1 Hz). ^{31}P NMR (C_6D_6 in ppm): δ 97.7 (s, 1P, $^1J_{Pt-P}$ = 3281 Hz), 260.9 (s, 1P, $^2J_{Pt-P}$ = 106 Hz). ES/MS: m/z = 1364. The d_2-isotopomer of **2**, $PtOs_3(CO)_7(PBu^t_3)(\mu\text{-}PBu^t_2)(\mu_4\text{-}CHCMeCH)(\mu\text{-}D)(D)$, was prepared in a similar manner by substituting D_2 for H_2 in the above synthesis.

Hydrogen Elimination from 2. A 5.0 mg (0.004 mmol) amount of **2** was dissolved in 8 mL of methylene chloride in a 25 mL three-neck flask. The solution was purged with nitrogen at room temperature for 5 h. The solvent was removed in vacuo and the residue was extracted with methylene chloride and separated by TLC using a 4:1 (v/v) solvent mixture of hexane/methylene chloride to yield in order of elution 1.2 mg (23%) of unreacted **2** and 2.9 mg of **1** (57%).

Reaction of 1 with Ph_3GeH. A 16.0 mg (0.012 mmol) amount of **1** was dissolved in 10 mL of distilled hexane in a 50 mL three-neck flask. Then 20.0 mg (0.066) of Ph_3GeH was added. The solution was allowed to stir at room temperature for 48 h. The solvent was then removed in vacuo and the residue was extracted with methylene chloride and separated by TLC using a 4:1 (v/v) solvent mixture of hexane/methylene chloride to yield in order of elution 10.3 mg (68%) of unreacted **1**, 0.5 mg (3%) of $PtOs_3(CO)_8(PBu^t_3)(\mu\text{-}PBu^t_2)(\mu_4\text{-}CHCMeCH)$,[11] and 2.0 mg (10%) of orange $PtOs_3(CO)_7(PBu^t_3)(\mu\text{-}PBu^t_2)(\mu_4\text{-}CHCMeCH)(GePh_3)(\mu\text{-}H)$, **3**. Spectral data for **3**: IR ν_{CO} (cm^{-1} in CH_2Cl_2): 2029(m), 1991(s, sh), 1985(vs), 1942(m, sh), 1932(m). ^{1}H NMR (C_6D_6 in ppm): δ −7.90 (dd, 1H, $^2J_{P-H}$ = 18 Hz, $^3J_{P-H}$ = 4 Hz), 1.20 (d, 9H, $^3J_{P-H}$ = 15 Hz), 1.30 (d, 9H, $^3J_{P-H}$ = 15 Hz), 1.38 (d, 27H, $^3J_{P-H}$ = 12 Hz), 3.28 (s, 3H), 5.63 (dd, 1H, $^3J_{P-H}$ = 13 Hz, $^4J_{P-H}$ = 1 Hz), 7.16 (m, 15H), 8.01 (d, 1H, $^3J_{P-H}$ = 6 Hz). ^{31}P NMR (C_6D_6 in ppm): δ 93.7 (s, 1P, $^1J_{Pt-P}$ = 2370 Hz), 132.6 (s, 1P). ES/MS: M^+ = 1668.

Reaction of 1 with Phenylacetylene. An 11.0 mg (0.008 mmol) amount of **1** was dissolved in 10 mL of distilled hexane in a three-neck flask. Then 0.01 mL (0.09 mmol) of phenylacetylene was

(11) Adams, R. D.; Boswell, E. *Organometallics* **2008**, *27*, 2021–2029.

Table 1. Crystallographic Data for Compounds 2−4

	2	3	4
empirical formula	$PtOs_3P_2O_7C_{31}H_{52}$	$PtOs_3GeP_2O_7C_{49}H_{66}\cdot 2C_6H_6$	$Os_3PO_7C_{27}H_{29}$
fw	1364.36	1667.45	1067.07
cryst syst	triclinic	monoclinic	triclinic
lattice params			
a (Å)	8.8502(8)	17.504(1)	9.0338(8)
b (Å)	13.743(2)	19.019(1)	10.6320(9)
c (Å)	15.624(3)	19.541(1)	15.838(4)
α (deg)	95.218(2)	90	79.472(2)
β (deg)	95.758(2)	102.623(1)	82.389(2)
γ (deg)	101.060(2)	90	84.241(2)
V (Å^3)	1843.8(3)	6347.9(6)	1478.0(2)
space group	$P\bar{1}$ (#2)	$P2_1/n$ (#14)	$P\bar{1}$ (#2)
Z value	2	4	2
ρ_{calc} (g/cm^3)	2.458	1.908	2.398
μ (Mo Kα) (mm^{-1})	14.214	8.745	12.959
temperature (K)	100(2)	294(2)	293(2)
$2\theta_{max}$ (deg)	51.38	56.96	56.88
no. obsd ($I > 2\sigma(I)$)	8350	11 540	5980
no. params	417	606	363
goodness of fit, GOF[a]	1.050	1.061	1.044
Max. shift in cycle	0.001	0.001	0.001
Residuals:[a] R1; wR2	0.0349; 0.0982	0.0435; 0.1034	0.0403; 0.1005
absorp correction, max./min.	multi-scan 1.000/0.267	multi-scan 1.000/0.560	multi-scan 1.000/0.438
largest peak in final diff map (e$^-$/Å^3)	1.854	3.005	2.645

[a] $R = \sum_{hkl}(||F_{obs}| - |F_{calc}||)/\sum_{hkl}|F_{obs}|$; $R_w = [\sum_{hkl}w(|F_{obs}| - |F_{calc}|)^2/\sum_{hkl}wF_{obs}^2]^{1/2}$, $w = 1/\sigma^2(F_{obs})$; GOF $= [\sum_{hkl}w(|F_{obs}| - |F_{calc}|)^2/(n_{data} - n_{vari})]^{1/2}$.

added via syringe. The solution was allowed to stir at room temperature for 24 h. The solvent was then removed in vacuo and the residue was extracted with methylene chloride and separated by TLC using a 4:1 (v/v) solvent mixture of hexane/methylene chloride to yield in order of elution 3.1 mg (35%) of yellow $Os_3(CO)_7(\mu\text{-}PBu^t_2)[\mu_3\text{-}CHCMeC(H)CCPhH]$, **4**, 2.0 mg (18%) of unreacted **1**, and 1.1 mg (9%) of $PtOs_3(CO)_8(PBu^t_3)(\mu\text{-}PBu^t_2)(\mu_4\text{-}CHCMeCH)$.[11] Spectral data for **4**: IR ν_{CO} (cm^{-1} in CH_2Cl_2): 2061(s), 2012(s, sh), 2001(vs), 1984(m), 1947(m). ^{1}H NMR ($C_6D_5CD_3$ in ppm at 25 °C): δ 1.00(d, 9H, $^3J_{P-H} = 15$ Hz), 2.15 (d, 3H, $^4J_{P-H} = 1$ Hz), 3.43 (d, 1H, $^3J_{P-H} = 2$ Hz), 6.84 (s, 1H), 7.062 (m, 5H), 7.84 (d, 1H, $^3J_{P-H} = 2$ Hz). ^{1}H NMR ($C_6D_5CD_3$ in ppm at 105 °C): δ 1.22 (d, 9H, $^3J_{P-H} = 14$ Hz), 1.36 (d, 9H, $^3J_{P-H} = 15$ Hz), 2.67 (d, 3H, $^4J_{P-H} = 1$ Hz), 3.51 (d, 1H, $^3J_{P-H} = 2$ Hz), 6.49 (s, 1H), 7.06 (m, 5H), 7.95 (d, 1H, $^3J_{P-H} = 1$ Hz). ^{31}P NMR (CD_2Cl_2 in ppm): δ 210.5 (s, 1P). EI/MS: 1068, M; 1040, M − CO; 1012, M − 2CO; 956, M − 4CO.

Crystallographic Analyses. Orange crystals of **2** suitable for diffraction analysis were grown under an H_2 atmosphere from a hexane solution at −25 °C. Orange single crystals of **3** were grown by slow evaporation of solvent from a benzene/octane solution at 5 °C. Yellow single crystals of **4** were grown by slow evaporation of solvent from a benzene/octane solution at 5 °C. Each data crystal was glued onto the end of a thin glass fiber. X-ray intensity data were measured by using a Bruker SMART APEX CCD-based diffractometer with Mo Kα radiation ($\lambda = 0.71073$ Å). The raw data frames were integrated with the SAINT+ program by using a narrow-frame integration algorithm.[12] Corrections for the Lorentz and polarization effects were also applied by SAINT. An empirical absorption correction based on the multiple measurement of equivalent reflections was applied by using the program SADABS. All structures were solved by a combination of direct methods and difference Fourier syntheses and refined by full-matrix least-squares on F^2, by using the SHELXTL software package.[13] Unless indicated otherwise, all hydrogen atoms were placed in geometrically idealized positions and included as standard riding atoms. Crystal data, data collection parameters, and results of the analyses for compounds are listed in Table 1.

Compound **2** crystallized in the triclinic crystal system. Several crystals of **2** were surveyed, and all were found to be twinned. The crystal selected for data collection was composed of two domains. Identification of the twinning and derivation of the twin law, which transforms the indices of one domain into those of the other, were performed with the Bruker program Cell_Now.[18] The twin law is

$$\begin{pmatrix} -1 & 0 & 0 \\ 0.630 & 1 & 0.196 \\ 0 & 0 & -1 \end{pmatrix}$$

which corresponds to a 180° rotation about the reciprocal [010] axis. Integration of the twinned raw data frames was performed with SAINT+.[14] Reflection files for structure solution (SHELX HKLF 4 format) and twin refinement (SHELX HKLF 5 format) were created with TWINABS.[14] Final unit cell parameters were determined by least-squares refinement of 6100 strong reflections from both domains. Direct methods structure solution, difference Fourier calculations, and full-matrix least-squares refinement against F^2 were performed with SHELXTL.[13] The major twin fraction refined to 0.535(1). The space group $P\bar{1}$ was selected and confirmed by the successful solution and refinement of the structure. All non-hydrogen atoms were refined with anisotropic thermal parameters. The hydrido ligands were located and refined with isotropic thermal parameters, but the bridging ligand H(6) was refined with the Pt and Os to H bond distances constrained to 1.75 Å.

Compound **3** crystallized in the monoclinic crystal system. The systematic absences in the intensity data were consistent with the unique space group $P2_1/c$. Two molecules of benzene cocrystallized in the asymmetric unit and were refined using isotropic displacement parameters. All non-hydrogen atoms were refined with anisotropic thermal parameters. The hydrido ligand was located and refined with an isotropic thermal parameter.

Compound **4** crystallized in the triclinic crystal system. The space group $P\bar{1}$ was selected and confirmed by the successful refinement of the structure. The molecule exhibits a minor disorder that refined to 0.952(1)/0.048(1). The refined disorder model takes the form of a rotation of the entire molecule around a vector approximately through Os(1) and the Os(2)/Os(3) midpoint. Only the positions of two of the osmium atoms of the minor disorder component (Os(2A) and Os(3A)) could be located due its low population. The position

(12) *SAINT+* Version 6.2a; Bruker Analytical X-ray System, Inc.: Madison, WI, 2001.

(13) Sheldrick, G. M. *SHELXTL* Version 6.1; Bruker Analytical X-ray Systems, Inc.: Madison, WI, 1997.

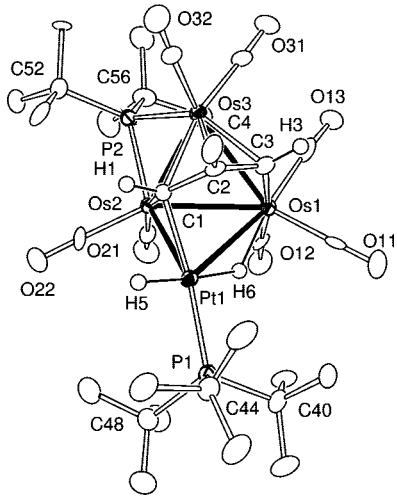

Figure 1. ORTEP diagram of **2** showing 65% thermal ellipsoid probability. Selected bond distances (A) and angles (deg) are as follows: Pt(1)−Os(2) = 2.7669(5), Pt(1)−Os(1) = 3.0829(5), Pt(1)−H(5) = 1.51(8), Pt(1)−H(6) = 1.75(2), Os(1)−C(3) = 2.119(8), Os(1)−Os(2) = 2.9201(5), Os(1)−Os(3) = 2.9631(5), Os(1)−H(6) = 1.75(2), Os(2)−C(1) = 2.226(7), Os(2)−P(2) = 2.290(2), Os(2)−Os(3) = 2.7339(5), Os(3)−C(3) = 2.239(8), Os(3)−C(2) = 2.263(8), Os(3)−P(2) = 2.352(2), Pt(1)−P(1) = 2.309(2), Os(3)−C(1) =2.353(8), C(1)−C(2) = 1.483(10), C(2)−C(3) = 1.412(11), Os(2)−Pt(1)−Os(1) = 59.599(11),Os(2)−Os(1)−Os(3) = 55.375(10), Os(2)−Os(1)−Pt(1) = 54.813(10), Os(3)−Os(1)−Pt-(1)=83.646(13),Os(3)−Os(2)−Pt(1)=94.291(14),Os(3)−Os(2)−Os(1) = 63.110(12), Pt(1)−Os(2)−Os(1) = 65.587(12).

of the third osmium atom of this group (Os(1A)) is coincident with Os(1). Refinement of the site occupancy (population) factors for Os(2A) and Os(3A) gave 0.050(1) and 0.051(2), respectively, with reasonable isotropic thermal parameters. The site occupancy factors for the major disorder component atoms Os(1), Os(2), and Os(3) were also refined and resulted in site occupancies of 1.00, 0.954(2), and 0.957(2), respectively. For the final refinement cycles, the total population of the major and minor components was constrained to sum to unity. The Os(1)/Os(1A) site was refined with a single set of atomic coordinates and displacement parameters. Os(2A) and Os(3A) were refined freely with isotropic thermal parameters. All other atoms were refined anisotropically. Because of the disorder, only the structure of the major disorder component is precisely determined. All non-hydrogen atoms were refined with anisotropic thermal parameters. All of the hydrogen atoms were calculated by assuming standard geometries and were included as fixed contributions on the final cycles of refinement.

Computational Treatments for 1 and 2. Calculations of **1** and **2** were performed by using density functional theory in the Gaussian 03 suite of ab initio programs.[15] The observed clusters were simplified to reduce computational demand. The two *tert*-butyl (^{t}Bu) groups on the P atom that is bonding to two Os atoms at a position above the active site were replaced by two methyl groups in the calculations. The ^{t}Bu groups on the P atom near the active site were retained. The location of the active site was determined in some preliminary calculations with all the ^{t}Bu groups replaced by methyl. The entire reaction pathway and relative energy barriers for each step were calculated with the meta-GGA nonempirical Tao−Perdew−Staroverov−Scuseria (TPSS) functional,[16] the correlation consistent polarized valence double-ζ (cc-pVDZ) basis set for the H, C, O, and P atoms,[17] and the Stuttgart relativistic small core ECP basis set (ECP60MWB) for the Os and Pt atoms.[18] Calculating the harmonic vibrational frequencies and noting the number of imaginary frequencies confirmed the structure of all intermediates (no imaginary frequency) and transition state (TS, only one imaginary frequency). TSs were also confirmed to connect

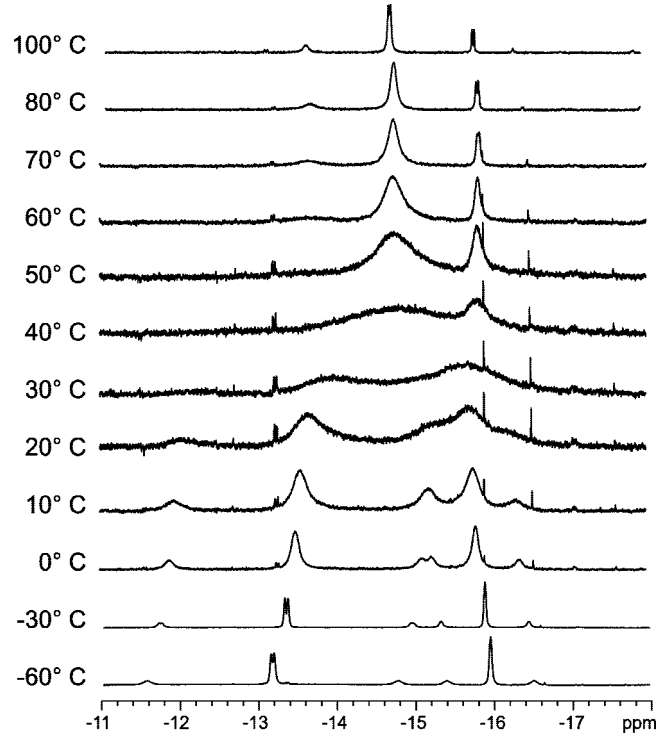

Figure 2. Variable-temperature ^{1}H NMR spectra of the hydride resonances of **2** recorded in d_8-toluene solvent.

reactants and products by intrinsic reaction coordinate (IRC) calculations. The effect of solvent was taken into account by performing reaction field calculations by using the integral equation formalism of the polarizable continuum models (IEF-PCM) for heptane (ε = 1.92). The zero-point energy (ZPE) and entropic contribution have been estimated within the harmonic potential approximation. The enthalpies, H, and free energies, G, were calculated for T = 298.15 K. All relative enthalpies and free energies are reported in kcal/mol, based on separated reagents $Os_3PtP(^tBu)_3$ and H_2 set equal to 0.0 kcal/mol. The molecular structure figures are drawn by using the JIMP2 molecular visualization and manipulation program.[19]

Computational Treatments for 3 and 4. Molecular orbital calculations for compounds **3** and **4** were performed by the Fenske−Hall method[20] by utilizing a graphical user interface developed[21] to build inputs and view outputs from stand-alone

(14) *SMART* Version 5.630, *Cell_Now*, *SAINT+* Version 6.45, and *TWINABS* Version 1.05; Bruker Analytical X-ray Systems, Inc.: Madison, WI, 2003.

(15) Frisch, M. J.; Trucks, G. W.; Schlegel, H. B.; Scuseria, G. E.; Robb, M. A.; Cheeseman, J. R.; Montgomery, J. A., Jr.; Vreven, T.; Kudin, K. N.; Burant, J. C.; Millam, J. M.; Iyengar, S. S.; Tomasi, J.; Barone, V.; Mennucci, B.; Cossi, M.; Scalmani, G.; Rega, N.; Petersson, G. A.; Nakatsuji, H.; Hada, M.; Ehara, M.; Toyota, K.; Fukuda, R.; Hasegawa, J.; Ishida, M.; Nakajima, T.; Honda, Y.; Kitao, O.; Nakai, H.; Klene, M.; Li, X.; Knox, J. E.; Hratchian, H. P.; Cross, J. B.; Adamo, C.; Jaramillo, J.; Gomperts, R.; Stratmann, R. E.; Yazyev, O.; Austin, A. J.; Cammi, R.; Pomelli, C.; Ochterski, J. W.; Ayala, P. Y.; Morokuma, K.; Voth, G. A.; Salvador, P.; Dannenberg, J. J.; Zakrzewski, V. G.; Dapprich, S.; Daniels, A. D.; Strain, M. C.; Farkas, O.; Malick, D. K.; Rabuck, A. D.; Raghavachari, K.; Foresman, J. B.; Ortiz, J. V.; Cui, Q.; Baboul, A. G.; Clifford, S.; Cioslowski, J.; Stefanov, B. B.; Liu, G.; Liashenko, A.; Piskorz, P.; Komaromi, I.; Martin, R. L.; Fox, D. J.; Keith, T.; Al-Laham, M. A.; Peng, C. Y.; Nanayakkara, A.; Challacombe, M.; Gill, P. M. W.; Johnson, B.; Chen, W.; Wong, M. W.; Gonzalez, C.; Pople, J. A. *Gaussian 03, revision C.02, suite of programs for ab initio calculation*; Gaussian, Inc.: Wallingford, CT, 2004.

(16) Tao, J. M.; Perdew, J. P.; Staroverov, V. N.; Scuseria, G. E. *Phys. Rev. Lett.* **2003**, *91*, 146401–146404.

(17) (a) Dunning, T. H., Jr. *J. Chem. Phys.* **1989**, *90*, 1007–1023. (b) Woon, D. E.; Dunning, T. H., Jr. *J. Chem. Phys.* **1993**, *98*, 1358–1371.

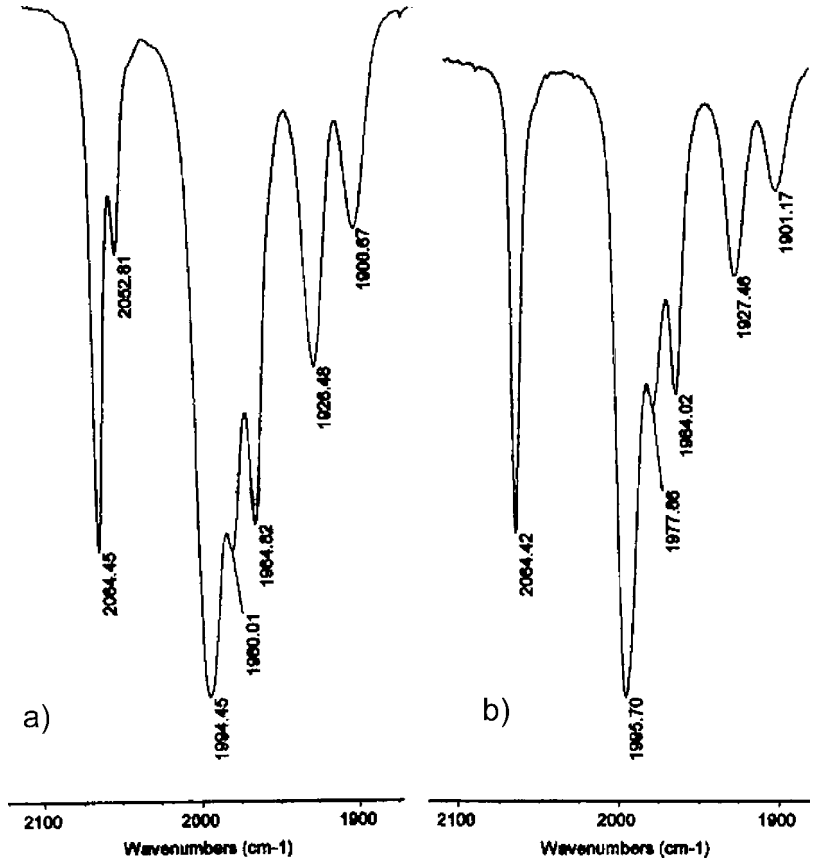

Figure 3. Infrared spectra of compounds **2** (a) and **2-*d*$_2$** (b) in the CO stretching region. Note the absence of the absorption 2052.8 cm^{-1} in spectrum b.

Scheme 1. Mechanism for the Intramolecular Exchange of the Hydrido Ligands in 2

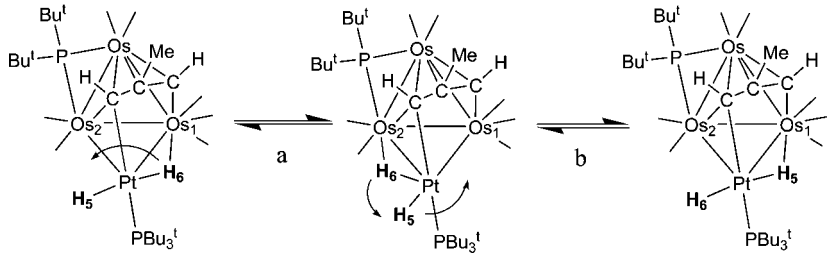

Fenske−Hall (version 0.1.v117) and MOPLOT2[22] binary executables. Contracted Clementi double-ζ basis sets were used for the Os 5d, Pt 5d, P 3p, and C and O 2p atomic orbitals. The Fenske−Hall scheme is a nonempirical, approximate method that is capable of calculating molecular orbitals for very heavy transition metal systems and has built-in fragment analysis routines that also allow one to assemble transition metal cluster structures from the ligand containing fragments. In these calculations, PH_3 was used in place of the PBu^t_3 ligand, PH_2 was used in place of the bridging PBu^t_2 ligand, P−H = 1.41 Å, and the methyl group on the bridging CHCMeCH ligand was replaced with a hydrogen atom with C−H = 0.95 Å. C(48) on **4** was also replaced with a hydrogen atom with C−H = 0.95 Å.

Results and Discussion

Compound **1** reacts with H_2 at room temperature to yield the compound $PtOs_3(CO)_7(PBu^t_3)(\mu\text{-}PBu^t_2)(\mu_4\text{-}CHCMeCH)(\mu\text{-}H)(H)$, **2**, in a 72% isolated yield. The conversion appears to be 100% spectroscopically, but the product loses H_2 during workup (see below), which results in a lower isolated yield. Compound **2** was characterized by a combination of IR and NMR spectroscopy, mass spectrometry, and single-crystal X-ray diffraction analysis. An ORTEP diagram of the molecular structure of **2** is shown in Figure 1. The structure of compound **2** is similar to that of **1**,[11] except that it contains two hydrido ligands. The four metal atoms exhibit the butterfly structure with the platinum atom in a wingtip site. Both hydrido ligands are bonded to the platinum atom. H(5) is a terminally coordinated ligand [Pt(1)−H(5) = 1.51(8) Å], while H(6) is a bridging ligand across the Pt(1)−Os(1) bond [Pt(1)−H(6) = Os(1)−H(6) = 1.75(2) Å]. The Pt(1)−Os(1) bond distance, 3.0829(5) Å, is significantly longer than the Pt(1)−Os(2) bond distance, 2.7669(5) Å, because of the presence of the bridging hydrido ligand.[23] There are three osmium−osmium bonds in **2**. The Os(1)−Os(3) and Os(2)−Os(3) bonds are very similar to those in **1**;

(18) (a) Andrae, D.; Haeussermann, U.; Dolg, M.; Stoll, H.; Preuss, H. *Theor. Chim. Acta* **1990**, *77*, 123–141. (b) Martin, J. M. L.; Sundermann, A. *J. Chem. Phys.* **2001**, *114*, 3408–3420.

(19) (a) *JIMP2*, version 0.091, a free program for visualizing and manipulating molecules: Hall, M. B.; Fenske, R. F. *Inorg. Chem.* **1972**, *11*, 768–779. (b) Manson, J.; Webster, C. E.; Hall, M. B. Texas A&M University, College Station, TX, 2006; http://www.chem.tamu.edu/jimp2/index.html.

Scheme 2. Predicted Reaction Mechanism and Relative Free Energies with Solvent Effect Corrections for the Activation of Hydrogen by Complex 1

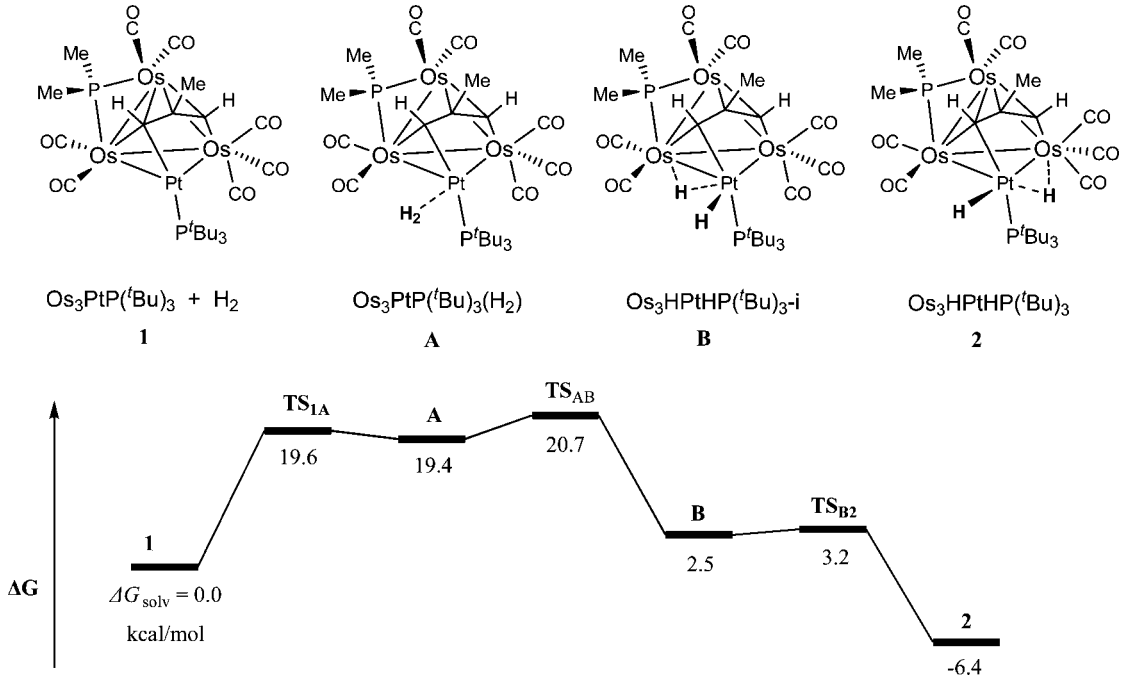

Os(1)−Os(3) = 2.9631(1) Å and Os(2)−Os(3) = 2.7339(1) Å. The latter is shorter than the former due to the presence of a bridging PBu^t_2 ligand. The Os(1)−Os(2) bond in **2**, 2.9201(1) Å, is slightly longer than that in **1**, 2.8767(3) Å. As in **1**, there is a quadruply bridging CHCMeCH ligand in the fold of the butterfly cluster. Atom C(1) is bonded to three metal atoms: Pt(1)−C(1) = 2.136(7) Å, Os(2)−C(1) = 2.226(7) Å, and Os(3)−C(1) =2.353(8) Å. C(2) is bonded only to Os(3) [Os(3)−C(2) = 2.263(8) Å], and C(3) bridges Os(1) and Os(3) [Os(1)−C(3) = 2.119(8) Å and Os(3)−C(3) = 2.239(8) Å]. The C−C bonds in the CHCMeCH ligand are significantly different; C(1)−C(2) = 1.483(10) Å, C(2)−C(3) = 1.412(11) Å. The short distance of the latter bond may be an indication of some C−C multiple bond character.

The hydrido ligands in **2** appear as two broad singlets located at $\delta = -15.8$ and -13.7 in the ^{1}H NMR spectrum at 20 °C. Suspecting dynamical activity, a series of ^{1}H NMR spectra of **2** was recorded at different temperatures. The ^{1}H NMR spectra of **2** as a function of temperature are shown in Figure 2. At −60 °C, the hydride resonances appear as a sharp doublet at $\delta = -12.82$, $^2J_{P-H} = 16$ Hz with strong coupling to ^{195}Pt ($^1J_{Pt-H} = 1285$ Hz) and a sharp singlet at $\delta = -15.62$ with smaller coupling to ^{195}Pt ($^1J_{Pt-H} = 443$ Hz). As the temperature is raised, the two resonances broaden, coalesce, and re-form as a sharp doublet at $\delta = -14.5$ ($^1J_{Pt-H} = 872$ Hz, $^2J_{P-H} = 10$ Hz) at 100 °C. From the coalescence temperature 40 °C, it is possible to calculate the $\Delta G^{\ddagger}$ of activation for the exchange process, which is 13.9(2) kcal/mol at 313 K. Clearly, the two hydride ligands are exchanging their sites rapidly on the NMR time scale at the higher temperatures, and the observation of Pt−H coupling in the fast exchange region confirms that this process occurs intramolecularly, i.e., without dissociation as H^+ or any other H-dissociative process. A two-step mechanism proposed for this is shown in Scheme 1. In the first step (a) the bridging

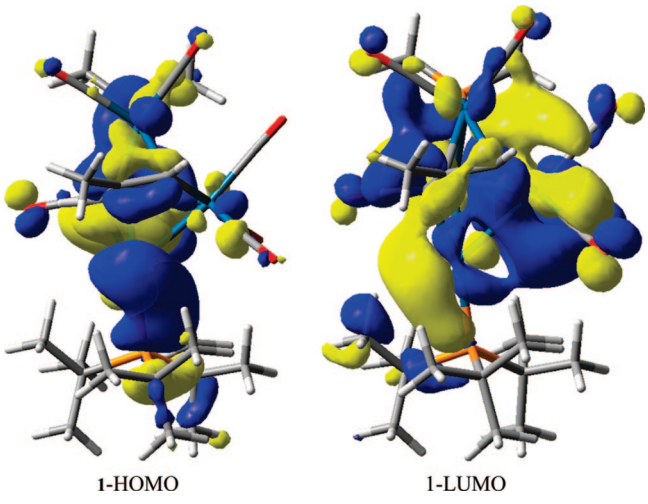

Figure 4. Contour diagrams of the HOMO (left) and LUMO (right) of **1**.

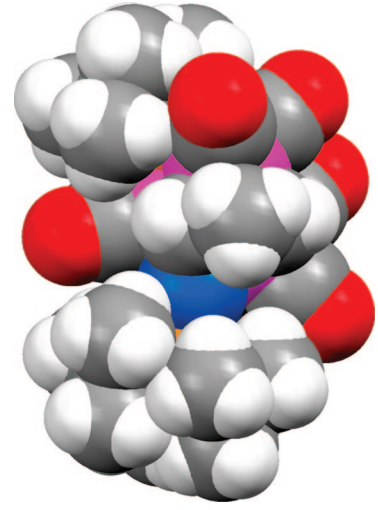

Figure 5. Space-filling model of **1** showing the accessibility of the platinum atom (blue) to approaches by H_2 through the ligand sphere.

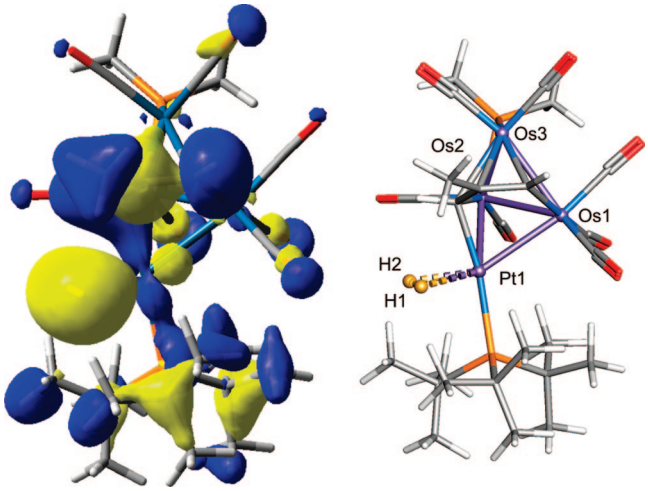

Figure 6. Contour diagram of the orbital showing the bonding of H_2 to **1** in the **1·H₂** adduct (left) and a stick drawing of the corresponding optimized structure of this unstable intermediate (right) showing the sideways interaction of the H_2 molecule (gold) with the platinum atom (blue).

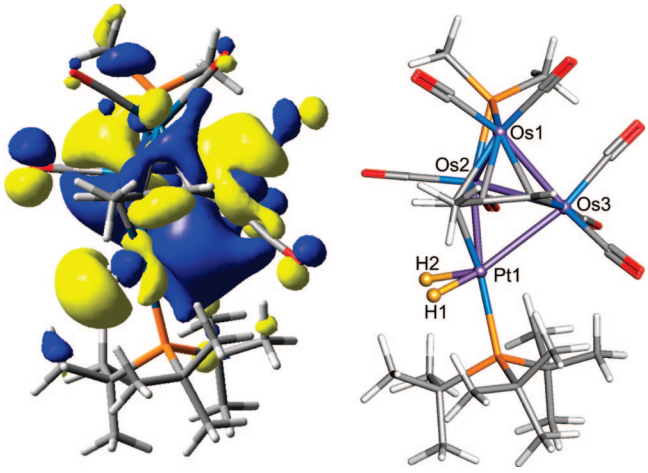

Figure 7. Contour diagram of the evolving H–H orbital (left) in the bond-breaking transition state $\mathbf{TS_{AB}}$ and a stick drawing of the corresponding optimized structure for H_2 splitting (right) with H atoms shown in gold.

hydrido ligand H(6) is shifted to the Pt−Os(2) bond. Support for this was obtained from the DFT computational analysis of **2** (see below), which indicated that the hydride shift of the bridging hydride ligand between the two Pt−Os bonds has a low barrier. In the second step H(5) is shifted from its terminal position to the bridging position across the Pt−Os(1) bond and H(6) is shifted to the terminal position on the platinum, as shown by the arrows on the intermediate in the scheme.

The Pt−H stretching vibration of the terminal hydride ligand H(5) was located in the infrared spectrum at 2053 cm^{-1}; see Figure 3a. Its distinction from the CO absorptions was confirmed by preparing the d_2-isomer of **2**, **2-*d*₂**, and recording its IR spectrum. Accordingly, the absorption at 2053 cm^{-1} was completely absent in the spectrum of **2-*d*₂**; see Figure 3b. Significantly, the addition of H_2 to **1** is reversible at room temperature. When purged with nitrogen for 5 h at 25 °C, compound **2** was converted back to **1** in 57% yield.

Because of the unusual facility and reversibility of the addition of H_2 to **1**, it was decided to investigate the mechanism of the H_2 addition to **1** by the use of DFT calculations. An energy level diagram of the profile of this reaction is shown in Scheme 2. Two intermediates and three transition states were found in the course of the calculations. Compound **1** activates H_2 by an oxidative-addition mechanism. The H_2 activation occurs at the platinum atom. To start, the HOMO and LUMO of **1** are shown in Figure 4. The LUMO of **1** clearly shows a pocket of unsaturation concentrated on the platinum atom.[11] A molecule of H_2 can approach the platinum atom in an open area in the ligand framework. A space-filling model of **1** is shown in Figure 5, which shows the accessibility of the platinum atom to direct approaches by H_2. The H_2 passes over the transition state $\mathbf{TS_{1A}}$, having a free energy barrier of 19.6 kcal/mol, and then forms an unstable dihydrogen adduct, intermediate **A**. A contour diagram of the key orbital of **A** that shows a bonding interaction of the H_2 molecule to the platinum atom in this geometry-optimized intermediate is shown in Figure 6. The coordination of the H_2 molecule is similar to the well-characterized "nonclassical" sideways bonding mode that has been observed in mononuclear metal complexes and has been thoroughly analyzed by theoretical methods.[5] A similar intermediate was indicated in a computational analysis of the addition of H_2 to the compound $Pt_2Re_2(CO)_7(PBu^t_3)_2(\mu\text{-}H)_2$.[7] The H−H bond is easily cleaved ($\Delta G = 1.3$ kcal/mol) passing over the transition state $\mathbf{TS_{AB}}$ (Figure 7) and forms an unstable intermediate **B**, which has one hydrido ligand terminally coordinated to platinum and one bridging hydrido ligand across the Pt−Os(2) bond. Figure

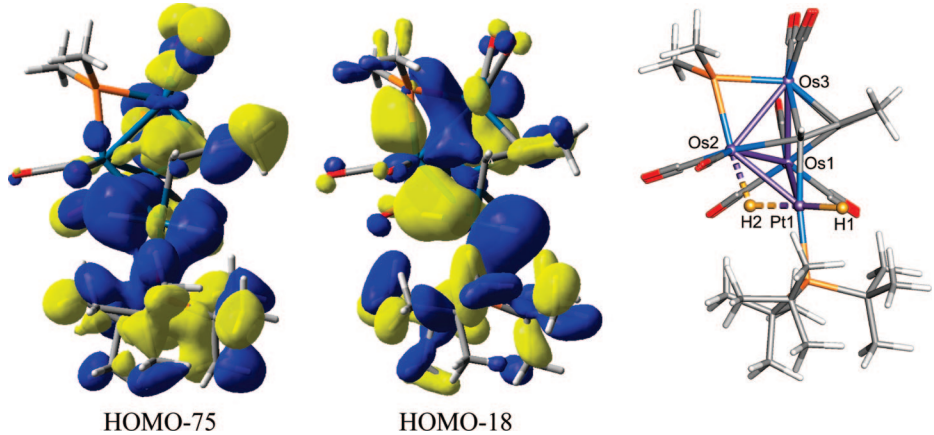

Figure 8. Contour diagrams of two orbitals, HOMO−75 (left) and HOMO−18 (center), that show the bonding of the terminal Pt−H and bridging Pt−H−Os bonding orbitals of the DFT-optimized structure of the intermediate **B**. On the right is a stick diagram that shows the precise locations of the hydrido ligands in these orbitals in **B**.

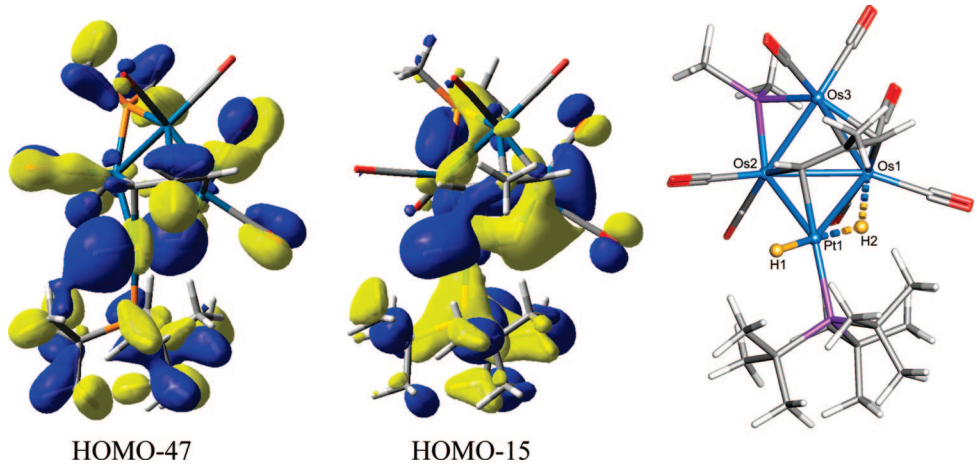

Figure 9. Contour diagrams of two orbitals, HOMO−47 (left) and HOMO−15 (center), that show the terminal Pt−H and bridging Pt−H−Os bonding interactions of the DFT geometry-optimized structure of **2**. On the right is a stick diagram view of **2** that shows the precise locations of the hydrido ligands in these orbitals.

8 shows contour diagrams of two molecular orbitals in **B** that show the bonding of the hydrido ligands to the metal atoms. As expected, the bridging hydrido ligand can be shifted readily from the Pt−Os(2) bond to a bridging site on the Pt−Os(1) bond to give the final product **2** through the transition state $\mathbf{TS_{B2}}$. The structure of **2** is 8.9 kcal/mol lower in free energy than that of **B**. The greater stability of **2** is consistent with its observation as the product of the reaction of H_2 with **1**. Contour diagrams of two molecular orbitals, HOMO−47 and HOMO−15, that show the bonding interactions of the terminal and bridging hydrido ligands of the DFT-optimized structure of **2** are shown in Figure 9.

The frequency calculations on **2** produced three Pt−H vibrational frequencies that are slightly coupled to some other vibrations. The most intense vibration by at least an order of magnitude is a Pt−H vibration at 2036 cm^{-1}, in which both hydrogen atoms move in the same direction and are coupled to all the C−O bond vibrations. This frequency is very close to an experimentally observed Pt−H vibrational frequency at 2053 cm^{-1}; see Figure 3. Two other very weak M−H vibrations are predicted, one at higher frequency, 2280 cm^{-1}, which comes mainly from the vibration of Pt with the terminal H, and another at lower frequency 1639 cm^{-1}, whichcomes mainly from the vibration of the bridging H between Pt and Os. Both of these two vibrations are coupled to each other, and the lower frequency one involves an H−Pt−H angle deformation. These two weaker vibrations were not observed experimentally.

Compound **1** reacts with $HGePh_3$ at room temperature to yield the compound $PtOs_3(CO)_7(PBu^t_3)(\mu\text{-}PBu^t_2)(\mu_4\text{-}CHCMeCH)(GePh_3)(\mu\text{-}H)$, **3**, in a low yield (10%). Compound **3** was characterized by a combination of IR and NMR spectroscopy, mass spectrometry, and single-crystal X-ray diffraction analysis. An ORTEP diagram of the molecular structure of **3** is shown

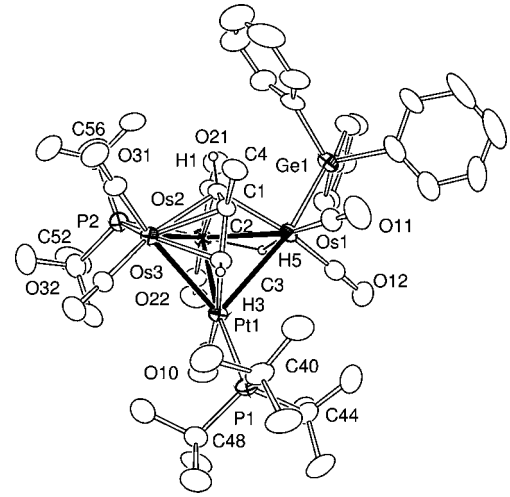

Figure 10. ORTEP diagram of **3** showing 30% thermal ellipsoid probability. Selected bond distances (A) and angles (deg) are as follows: Pt(1)−Os(3) = 2.8654(4), Pt(1)−Os(2) = 2.8716(4), Pt(1)−Os(1) = 2.9611(4), Os(1)−Os(2) = 2.8490(4), Os(2)−Os(3) = 2.8357(4), Os(1)−Ge(1) = 2.4933(9), Os(1)−H(5) = 1.76(2), Os(2)−C(1) = 2.207(7), Pt(1)−C(3) = 2.046(7), Os(1)−H(5) = 1.76(2), Os(2)−H(5) = 1.73(2), Os(3)−C(3) = 2.219(7), Os(3)−C(2) = 2.284(7), Os(1)−C(2) = 2.417(7), Os(3)−C(1) = 2.315(8), Pt(1)−P(1) = 2.4673(19), Os(2)−P(2) = 2.411(2), Os(3)−P(2) = 2.3258(19), C(1)−C(2) = 1.438(10), C(2)−C(3) = 1.433(10); Os(3)−Pt(1)−Os(2) = 59.246(9), Os(3)−Pt(1)−Os(1) = 84.043(12), Os(2)−Pt(1)−Os(1) = 58.455(10), Os(2)−Os(1)−Pt(1) = 59.202-(9), Os(3)−Os(2)−Os(1) = 86.662(12), Os(3)−Os(2)−Pt(1) = 60.269(10), Os(1)−Os(2)−Pt(1) = 62.343(10).

in Figure 10. The structure of **3** is slightly different from that of **1**. It still contains a butterfly arrangement of four metal atoms. However, there has been a rearrangement of the metal−metal bonding. In **3**, the platinum atom occupies a "hinge" site of the butterfly and is bonded to all three osmium atoms, Pt(1)−Os(3) = 2.8654(4) Å, Pt(1)−Os(2) = 2.8716(4) Å, Pt(1)−Os(1) = 2.9611(4) Å. There are only two Os−Os bonds: Os(1)−Os(2) = 2.8490(4) Å and Os(2)−Os(3) = 2.8357(4) Å. The Os(1)···Os(3) distance, 3.901(1) Å, is too long to have a significant direct bonding interaction. There is a triphenylgermyl ligand bonded to Os(1); Os(1)−Ge(1) = 2.4933(9) Å. There is a quadruply bridging CHCMeCH ligand in the fold of this cluster, but in this complex the atom C(1) is bonded to three osmium atoms: Os(1)−C(1) = 2.264(7) Å, Os(2)−C(1) =

(20) (a) Hall, M. B.; Fenske, R. F. *Inorg. Chem.* **1972**, *11*, 768–775. (b) Webster, C. E.; Hall, M. B. In *Theory and Applications of Computational Chemistry: The First Forty Years*; Dykstra, C. Ed.; Elsevier: Amsterdam, 2005; Chapter 40, pp 1143−1165.

(21) Manson, J.; Webster, C. E.; Hall, M. B. *JIMP* Development Version 0.1.v117 (built for Windows PC and Redhat Linux); Department of Chemistry, Texas A&M University, College Station, TX 77842 (http://www.chem.tamu.edu/jimp/).

(22) MOPLOT2: for orbital and density plots from linear combinations of Slater or Gaussian type orbitals; Version 2.0, June 1993; Lichtenberger, D. L., Department of Chemistry, University of Arizona, Tucson, AZ 85721.

(23) (a) Bau, R.; Drabnis, M. H. *Inorg. Chim. Acta* **1997**, *259*, 27–50. (b) Teller, R. G.; Bau, R. *Struct. Bonding (Berlin)* **1981**, *44*, 1–82.

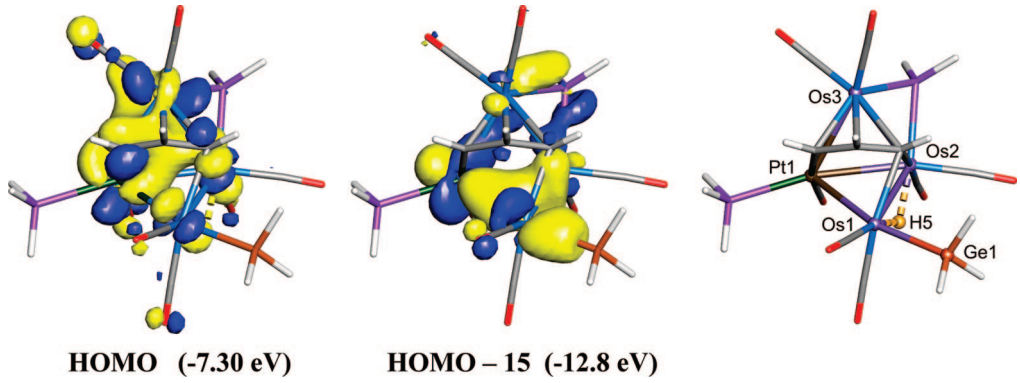

Figure 11. Contour diagrams of the Fenske−Hall HOMO (left) and HOMO−15 (center) of **3**. Stick diagram on the right shows the orientation of the molecule used in the contour diagrams.

2.207(7) Å, and Os(3)−C(1) = 2.315(8) Å. C(2) is bonded only to Os(3) [Os(3)−C(2) = 2.284(7) Å], and C(3) bridges Pt(1) and Os(3) [Pt(1)−C(3) = 2.046(7) Å and Os(3)−C(3) = 2.219(7) Å]. The C−C bond distances in the CHCMeCH ligand are not significantly different in this complex; C(1)−C(2) = 1.438(10) Å, C(2)−C(3) = 1.433(10) Å. There is one hydrido ligand, H(5), that was located and refined in the analysis. It bridges the Os(1)−Os(2) bond; Os(1)−H(5) = 1.76(2) Å and Os(2)−H(5) = 1.73(2) Å. A PBu^t_2 ligand bridges the Os(2)−Os(3) bond; Os(2)−P(2) = 2.411(2) Å and Os(3)−P(2) = 2.3258(19) Å. Unlike **2**, there is a terminal CO ligand coordinated to the platinum atom of **3** and the atom Os(1) has only two carbonyl ligands. It appears that the addition of Ph_3GeH to **1** was preceded by a shift of one of the CO ligands on Os(1) to the platinum atom, which in turn created a "vacant" site at that osmium atom, so that the oxidative-addition of the GeH bond of the $HGePh_3$ molecule can then occur there. The reason for the different site of addition for $HGePh_3$ is probably steric. The H_2 molecule is very small and can penetrate the coordination sphere around the platinum atom in **1** without the need of a ligand rearrangement. However, $HGePh_3$ is very bulky and evidently cannot add there due to the presence of the very bulky PBu^t_3 ligand, so the $HGePh_3$ addition occurs at the sterically more accessible neighboring osmium atom. However, the platinum atom is not an innocent spectator in this change of mechanism. Indeed, it was the shift of the CO ligand from the osmium atom to that platinum atom that created the vacant site and thus made the addition to the osmium atom possible. It has been shown in other studies that $Pt(PBu^t_3)$ groups can facilitate the formation of phosphine-substituted derivatives of $Os_3(CO)_{12}$ by assisting in the removal of the CO ligands form the osmium atoms.[24]

In order to understand the bonding in **3**, Fenske−Hall molecular orbitals were calculated. The frontier orbitals for **3** are shown in Figure 11. The HOMO lies at −7.30 eV and consists mostly of metal−metal bonding delocalized across the four metal atoms in the cluster. To see the effect of the bonding of the $GePh_3$ and hydrido ligands, one must look at orbitals at lower energies. HOMO−15 lies at −12.8 eV and shows both Os−Ge bonding along with some Os(1)−H(5) and Os(2)−H(5) bonding. This orbital also shows strong metal−metal interactions. The yield of **3** is low, and much of the starting material is recovered. However, attempts to increase the yield by heating this reaction under reflux for 24 h in hexane did not increase the yield. Attempts to perform the reaction at higher temperatures, i.e., octane, did not yield any **3** at all, but gave only trace amounts of other uncharacterizable products.

Compound **1** also reacts with phenylacetylene at room temperature to give the new compound $Os_3(CO)_7(\mu\text{-}PBu^t_2)[\mu_3\text{-}\eta^5$-CHCMeC(H)CCPhH], **4**, in a 35% yield. Compound **4** was characterized by a combination of IR and NMR spectroscopy, mass spectrometry, and single-crystal X-ray diffraction analysis. An ORTEP diagram of the molecular structure of **4** is shown in Figure 12. Compound **4** contains only three metal atoms, all of osmium. The three osmium atoms are mutually bonded, but the Os−Os distances are all significantly different; Os(1)−Os(3) = 2.9784(4) Å, Os(1)−Os(2) = 2.9209(4) Å, and Os(2)−Os(3) = 2.8080(4) Å. The Os(2)−Os(3) bond is significantly shorter than the other Os−Os bonds, because it contains a bridging PBu^t_2 ligand. Compound **4** has added 1 equiv of PhC_2H and eliminated the entire $Pt(PBu^t_3)$ group in the process. The elimination of $Pt(PBu^t_3)$ groups from metal cluster complexes has been observed on previous occasions.[24,25] In fact, the compounds $Os_3(CO)_{12}[Pt(PBu^t_3)]_n$, n = 1−3, readily interconvert in solution at room temperature by exchange of their $Pt(PBu^t_3)$ groups.[24] The $Pt(PBu^t_3)$ group in the compound $PtRu_5(CO)_{13}(PBu^t_3)(\mu_3\text{-}PhC_2H)(\mu_5\text{-}C)$ was cleaved from the cluster upon reaction with PhC_2H.[25] In the addition of the PhC_2H molecule to **1** the hydrogen atom was shifted to the phenyl-substituted carbon atom to form a C═C(H)Ph group and the unsubstituted carbon atom then formed a bond to one of the

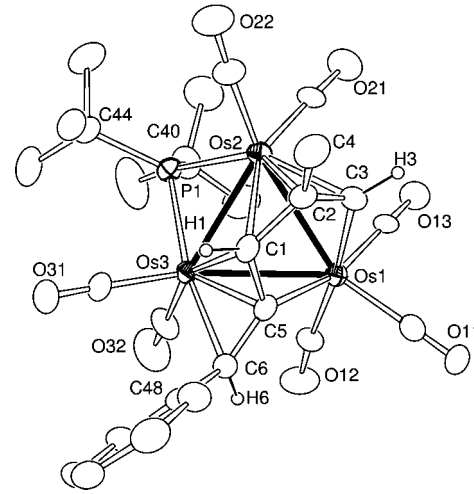

Figure 12. ORTEP diagram of **4** showing 30% thermal ellipsoid probability. Selected bond distances (A) are as follows: Os(1)−Os(2) = 2.9209(4), Os(1)−Os(3) = 2.9789(4), Os(2)−Os(3) = 2.8080(4), Os(1)−C(5) = 2.115(7), Os(1)−C(3) = 2.120(8), Os(2)−C(3) = 2.233(8), Os(2)−C(2) = 2.250(8), Os(2)−P(1) = 2.342(2), Os(2)−C(1) = 2.540(8), Os(3)−C(5) = 2.158(8), Os(3)−C(6) = 2.332(8), Os(3)−P(1) = 2.345(2), C(1)−C(2) = 1.451(11), C(1)−C(5) = 1.470(11), C(2)−C(3) = 1.406(12), C(2)−C(4) = 1.501(11), C(5)−C(6) = 1.381(11).

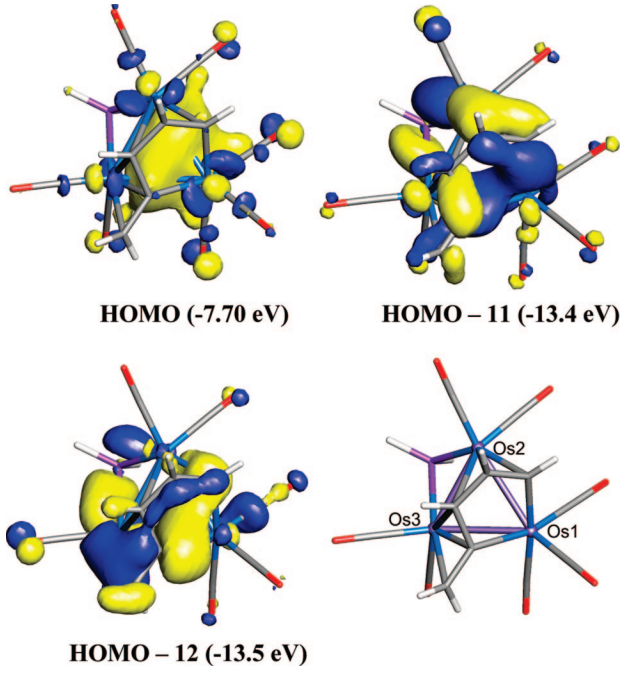

Figure 13. Contour diagrams of the Fenske−Hall HOMO (upper left), HOMO−11 (upper right), and HOMO−12 (lower left) of **4**. Stick diagram on the lower right shows the orientation of the molecule used in the contour diagrams.

CH groups of the HCC(Me)CH ligand present in **1**. The new μ_3-η^5-Ph(H)CCC(H)CMeCH ligand bridges all three osmium atoms. Atom C(5) bridges Os(1) and Os(3); Os(1)−C(5) = 2.115(7) Å and Os(3)−C(5) = 2.158(8) Å. C(6) is coordinated to Os(3) only; Os(3)−C(6) = 2.332(8) Å. The C(5)−C(6) bond distance is short, 1.38(1) Å, indicating the presence of some double-bond character. Atom C(3) bridges Os(1) and Os(2); Os(1)−C(3) = 2.120(8) Å, Os(2)−C(3) = 2.233(8) Å. Atom C(2) is coordinated to Os(2); Os(2)−C(2) = 2.250(8) Å. C(1) is about equidistant to Os(2) and Os(3), and both of these bonds are fairly long [Os(2)−C(1) = 2.540(8) Å and Os(3)−C(1) = 2.519(8) Å] and probably weak. At room temperature, the ^{1}H NMR spectrum of **4** shows only one resonance for the *tert*-butyl groups of the bridging PBu^t_2 ligand, δ = 1.00 (9H, $^3J_{P-H}$ = 15 Hz). The resonance of the other *tert*-butyl group is very broad due to a dynamical exchange process. However, at 105 °C, both *tert*-butyl resonances are observed, one at δ = 1.22 (9H, $^3J_{P-H}$ = 14 Hz) and the other at 1.36 (9H, $^3J_{P-H}$ = 15 Hz), and both are sharp. The spectral changes are due to a dynamical exchange process involving hindered rotation about the P−C bond, which renders the methyl groups inequivalent at low temperatures. This phenomenon is well documented in related systems that contain PBu^t groupings.[26]

A Fenske−Hall molecular orbital analysis of **4** was also performed. The frontier orbitals for **4** are shown in Figure 13. The HOMO lies at −7.70 eV and shows the nature of the delocalized metal−metal bonding between the osmium atoms. The delocalized bonding of the bridging Ph(H)CCC(H)CMeCH ligand is nicely displayed by the HOMO−11 and HOMO−12 orbitals, which lie at −13.4 and −13.5 eV, respectively. In its uncharged form, the μ_3-η^5-Ph(H)CCC(H)CMeCH ligand is a seven-electron donor. The PBu^t_2 group is a three-electron donor, and compound **4** thus achieves the closed-shell 48-electron configuration.

Scheme 3

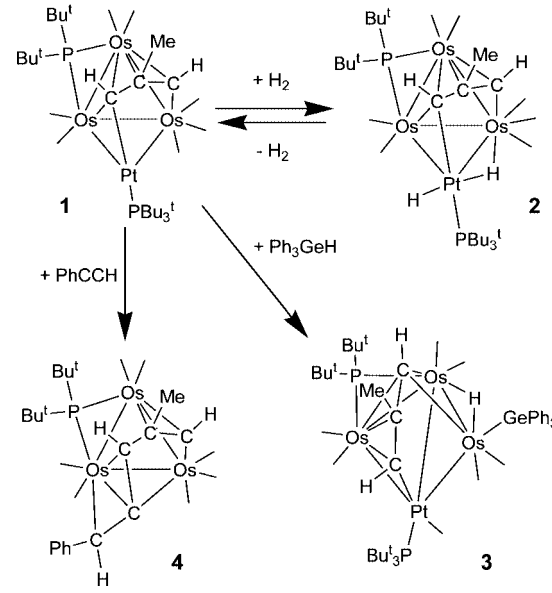

Summary

A summary of the reactions studied in this work is shown in Scheme 3. The unusual reactivity of **1** is intimately tied to its electronic unsaturation at the platinum atom, which is predicated on the presence of the very bulky PBu^t_3 ligand. Interestingly, compound **1** readily oxidatively adds H_2 reversibly under mild conditions to yield the dihydrido complex **2**. This addition occurs at the platinum atom. Compound **1** also adds triphenylgermane by oxidative-addition of its GeH bond, but this occurs at an osmium atom that is bonded to the platinum atom and a CO ligand is shifted from osmium to the platinum atom. Phenylacetylene adds to **1** at its HCCMeCH ligand to form a bridging Ph(H)CCC(H)CMeCH ligand, which is a seven-electron donor, but it loses the platinum atom with its phosphine ligand in the process.

Acknowledgment. This research was supported by the National Science Foundation (CHE-0743190 to R.D.A. and CHE-0518074 and CHE-0541587 to M.B.H.) and the Welch Foundation (A0648 to M.B.H.). We thank Dr. Mark D. Smith for assistance with the structural analyses and Dr. Perry Pellechia for assistance with the variable-temperature NMR spectra. This report is dedicated to the memory of Professor F. A. Cotton.

Supporting Information Available: CIF files for each of the structural analyses are available. This material is available free of charge via the Internet at http://pubs.acs.org.

OM800467V

(24) Adams, R. D.; Captain, B.; Zhu, L. *Inorg. Chem.* **2006**, *45*, 430–436.
(25) Adams, R. D.; Captain, B.; Zhu, L. *J. Organomet. Chem.* **2006**, *691*, 3122–3128.
(26) (a) Adams, R. D.; Captain, B.; Fu, W.; Pellechia, P. J.; Smith, M. D. *Inorg. Chem.* **2003**, *42*, 2094–2101. (b) Rithner, C. D.; Bushweller, C. H. *J. Am. Chem. Soc.* **1985**, *107*, 7823–7836. (c) Bushweller, C. H.; Brunelle, J. A. *J. Am. Chem. Soc.* **1973**, *95*, 5949–5955.